

CK-B chick
 CK sea ur2 IKPFSYD
 CK sea ur3
 CK-Mt chic
 GK ma.worm SISATASRHMTL

FIG. 3. Alignment of the amino acid sequences of 10 phosphagen kinases. This alignment was obtained with the algorithm of Feng & Doolittle [5]. Invariable residues are indicated by asterisks. The reactive cysteine is shown by \$. References; CK-M chick (chicken muscle isoform) [10, 14]; CK-B chick (chicken brain isoform) [7]; CK sea ur2 and 3 (domains 2 and 3 of sea urchin) [20]; CK-Mt chic (chicken mitochondrial isoform) [8]; GK ma.worm (*Neanthes*) [18]; AK shrimp (*Penaeus*) (this work); AK abalone (*Nordotis*) [18]; AK lobster (*Homarus*) [3]; PK Schis. 1 (domain 1 of *Schistosoma*) [15].

TABLE 2. Percent identity between the sequences of phosphagen kinases

	AK lob	AK aba	PK Sch	CK-M	CK-B	CK ur2	CK ur3	CK-Mt	GK wor
Ak shr	91.0	50.9	46.3	42.5	43.0	42.3	41.7	39.8	38.5
AK lob		52.6	45.7	41.8	41.8	41.7	41.7	39.3	38.8
AK aba			51.8	38.3	36.9	43.3	39.8	37.3	37.1
PK Sch				34.4	35.8	36.8	36.2	35.9	34.6
CK-M					80.3	68.2	65.2	67.2	53.2
CK-B						65.8	65.8	66.7	56.2
CK ur2							68.9	65.5	51.1
CK ur3								64.1	51.0
CK-MT									57.4

Abbreviations: shr, *Penaeus*; lob, *Homarus*; aba, *Nordotis*; Sch, domain 1 of *Schistosoma*; CK-M, chicken muscle isoform; CK-B, chicken brain isoform; ur2 and ur3, domains 2 and 3 of sea urchi; CK-Mt, chicken mitochondrial isoform; wor, *Neanthes*.

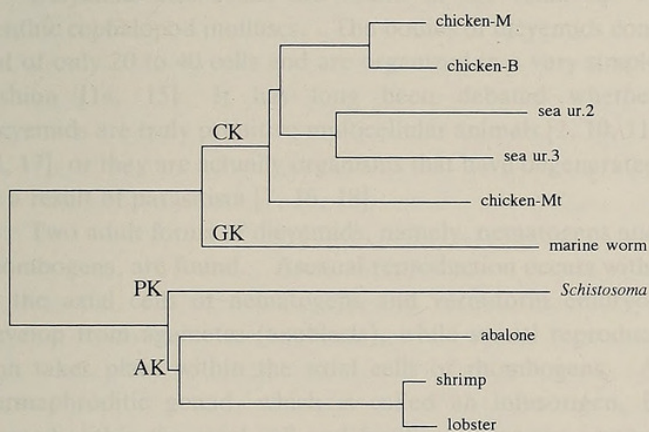


FIG. 4. A phylogenetic tree constructed from 10 sequences of phosphagen kinases aligned in Fig. 2. The tree was obtained with the program of Feng & Doolittle [5].

tions 13, 65-69, 198 and 265-268 in Fig. 3. Stein *et al.* [15] assigned tentatively *Schistosoma* PK as CK, based on the very weak, but reproducible CK activity in the crude extracts. However, since the enzyme activities of CK, GK, AK are strictly specific and those of TK, HTK, LK, OK and ThalK are more or less interspecific [1, 19], it is very likely that *Schistosoma* PK belongs to a member of the latter group. Dumas & Camonis [3] also suggest this possibility, based on the higher % identity between *Schistosoma* PK and lobster AK.

The evolutionary origin of phosphagen kinases is of

primary concern. Of the phosphagen kinases, AK is most widely distributed in animals. However the wide distribution does not imply that AK is closer to an ancestral phosphagen kinase. To solve this problem, we are planning to analyze the phosphagen kinases from more primitive animals, such as sea anemones and protozoa.

REFERENCES

- 1 Brevet A, Zeitoun Y, Pradel LA (1975) Comparative structural studies of the active site of ATP: guanidine phosphotransferases. The essential cysteine tryptic peptide of taurocyamine kinase from *Arenicola marina*. *Biochim Biophys Acta* 393: 1-9
- 2 Der Terrossian E, Desvages G, Pradel LA, Kassab R, Thoai NV (1971) Comparative structural studies of the active site of ATP: guanidine phosphotransferases. The essential cysteine tryptic peptide of lombricine kinase from *Lumbricus terrestris* muscle. *Eur J Biochem* 22: 585-592
- 3 Dumas C, Camonis J (1993) Cloning and sequence analysis of the cDNA for arginine kinase of lobster muscle. *J Biol Chem* 268: 21599-21605
- 4 Felsenstein J (1993) PHYLIP (Phylogeny Inference Package) version 3.5c Distributed by the author. Department of Genetics, University of Washington, Seattle, USA
- 5 Feng DA, Doolittle RF (1987) Progressive sequence alignment as a prerequisite to correct phylogenetic tree. *J Mol Evol* 25: 351-360
- 6 Furter R, Furter-Graves EM, Wallimann T (1993) Creatine kinase: The reactive cysteine is required for synergism but is nonessential for catalysis. *Biochemistry* 32: 7022-7029
- 7 Hossle JP, Rosenberg UB, Schafer B, Eppenberger HM, Perriard JC (1986) The primary structure of chicken B-creatine

- kinase and evidence for heterogeneity of its mRNA. *Nucl Acids Res* 14: 1449-1463
- 8 Hossle JP, Schlegel J, Wegmann G, Wyss M, Bohlen P, Eppenberger HM, Wallimann T, Perriard JC (1988) Distinct tissue specific mitochondrial creatine kinases from chicken brain and striated muscle with a conserve CK framework. *Biochem Biophys Res Commun* 151: 408-416
 - 9 Kenyon GL, Reed GH (1986) Creatine kinase: Structure-activity relationships. *Adv Enzymol* 54: 367-426
 - 10 Kwiatkowski RW, Schweinfest CW, Dottin RP (1984) Molecular cloning and the complete nucleotide sequence of the creatine kinase-M cDNA from chicken. *Nucl Acids Res* 12: 6925-6934
 - 11 Morrison JF (1973) Arginine kinase and other invertebrate guanidino kinases. In *The Enzymes*, vol. VIII (Ed by PC Boyer) Academic Press, New York and London, 457-486
 - 12 Okamoto S (1992) Primary structure of arginine kinase from *Penaeus japonicus* (in Japanese). *M Sci Thesis Kochi Univ*, Kochi, Japan
 - 13 Okamoto S, Iwasaki K, Furukohri T, Suzuki T (1991) Primary structure of arginine kinase from the tail muscle of the prawn *Penaeus japonicus*. *Zool Sci* 8: 1141 (Abstract)
 - 14 Ordahl CP, Evans GL, Cooper TA, Kunz G, Perriard JC (1984) Complete cDNA-derived amino acid sequence of chicken muscle creatine kinase. *J Biol Chem* 259: 15224-15227
 - 15 Stein LD, Harn DA, David JR (1990) A cloned ATP: Guanidino kinase in the trematode *Schistosoma mansoni* has a novel duplicated structure. *J Biol Chem* 265: 6582-6588
 - 16 Suzuki T (1986) Amino acid sequence of myoglobin from the mollusc *Dolabella auricularia*. *J Biol Chem* 261: 3692-3699
 - 17 Suzuki T (1994) Evolution of phosphagen kinase (II). PCR amplification of cDNAs of *Sulculus* and *Penaeus* arginine kinases with a universal phosphagen kinase primer. (in Japanese) *Mem Fac Sci Kochi Univ Ser D (Biology)* 15: 1-5
 - 18 Suzuki T, Furukohri T (1994) Evolution of phosphagen kinase. Primary structure of glycoamine kinase and arginine kinase from invertebrates. *J Mol Biol* in press
 - 19 Watts DC (1968) Variation in enzyme structure and function: The guidelines of evolution. *Adv Comp Physiol Biochem* 3: 1-115
 - 20 Wothe DD, Charbonneau H, Shapiro BM (1990) The phosphocreatine shuttle of sea urchin sperm: Flagellar creatine kinase resulted from gene triplication. *Proc. Natl. Acad. Sci USA* 87: 5203-5207

The Development of the Vermiform Embryos of Two Mesozoans, *Dicyema acuticephalum* and *Dicyema japonicum*

HIDETAKA FURUYA, KAZUHIKO TSUNEKI, and YUTAKA KOSHIDA¹

Department of Biology, College of General Education, Osaka University, Toyonaka 560, and ¹The National Center for University Entrance Examination, Tokyo 153, Japan.

ABSTRACT—The pattern of cell division and the cell lineage of the vermiform embryos of dicyemid mesozoans were studied under the light microscope using fixed and stained specimens of two species, namely, *Dicyema acuticephalum*, which has 16 to 18 peripheral cells, and *Dicyema japonicum*, which has 22 peripheral cells. An agamete first divides into two apparently equivalent daughter cells which remain in contact with one another. One of these cells becomes the mother cell of the head of the embryo. The other cell divides again equally to produce the prospective axial cell and the mother cell of the trunk and the tail of the embryo. The division proceeds spirally in the early stages but becomes bilateral from the fifth cell division onward. The embryo finally exhibits apparently bilateral symmetry. In two lines of cells, namely, those descended from the prospective axial cell and those from the mother cell of the head, extremely unequal divisions occur and the resultant, much smaller cells from each unequal division degenerate and ultimately disappear during embryogenesis. At the thirteen-cell stage, peripheral cells surround the prospective axial cell. At the final stage of embryogenesis, the prospective axial cell divides into two daughter cells. The anterior one is the axial cell itself and the posterior one is incorporated into the axial cell to form an agamete. Differences in numbers of peripheral cells are due to the number of times that divisions of the mother cells occur. The cell lineage of the calotte differs between *D. acuticephalum* and *D. japonicum*.

INTRODUCTION

Dicyemid mesozoans are found in the renal sac of benthic cephalopod molluscs. The bodies of dicyemids consist of only 20 to 40 cells and are organized in a very simple fashion [14, 15]. It has long been debated whether dicyemids are truly primitive multicellular animals [2, 10, 11, 13, 17], or they are actually organisms that have degenerated as a result of parasitism [7, 16, 18].

Two adult forms of dicyemids, namely, nematogens and rhombogens, are found. Asexual reproduction occurs within the axial cells of nematogens and vermiform embryos develop from agametes (axoblasts), while sexual reproduction takes place within the axial cells of rhombogens. A hermaphroditic gonad, which is called an infusorigen, is formed within the axial cell and fertilization occurs around the infusorigen. The zygote undergoes cleavages and develops into an infusoriform embryo within the axial cell. The processes of gametogenesis and cleavage have recently been described in detail [4, 5]. The development of vermiform embryos was described in the early literature [6, 8 cited in 14, 12, 14, 16], but the pattern of cell divisions and the process of cell arrangement during embryogenesis remain to be established. Moreover, cell lineages have not been completely characterized. In this report, we describe details of the development of the vermiform embryo of *Dicyema acuticephalum*, which has from 16 to 18 peripheral cells [16], and of *Dicyema japonicum*, which has 22 peripheral cells [3].

Dicyemids are examples of animals with a fixed cell number and their somatic cells undergo only a limited number of divisions during embryogenesis. The analysis of embryonic cell lineages in dicyemids is important since it provides clues towards an understanding of a simple or basic pattern of cell differentiation in multicellular animals.

MATERIALS AND METHODS

Forty-seven octopuses, *Octopus vulgaris*, were purchased or collected by the authors in the waters off the western coast of Japan. In this region, four species of dicyemids are found in the kidneys of *Octopus vulgaris* [3]. In this study, only *Dicyema acuticephalum* and *Dicyema japonicum* were examined.

After sacrifice, the renal sacs of each octopus were removed and smeared directly on glass slides. Smeared dicyemids were immediately fixed with Carnoy's fixative or with alcoholic Bouin's solution (a mixture of absolute ethanol saturated with picric acid, formalin and acetic acid, 15:5:1, v/v). Specimens fixed with Carnoy's fixative were stained with Feulgen's stain or by the PAS method and were poststained with Ehrlich's hematoxylin and light green. Specimens fixed with alcoholic Bouin's solution were stained with Ehrlich's hematoxylin and light green only. The embryos in the axial cells of nematogens were observed under a light microscope with an oil-immersion objective at a final magnification of 2,000 diameters. Cells were identified by various criteria, such as the position within the embryo, the size of the nucleus and the cell, and the stainability of the nucleus and the cell. Paying careful attention, we identified each swollen nucleus that was about to divide and each metaphase figure in terms of the cell that was going to divide and the resultant two daughter cells. Each developing embryo with or without dividing cells was sketched at three different optical depths and a three-dimensional diagrams were generated from these

sketches.

The early division of the vermiform embryos is somewhat spiral, but not absolutely so, and it proceeds cell by cell and not by quartets. Therefore, a new terminology was developed to describe the cells. Although the body of a vermiform specimen does not differentiate into a dorsal and a ventral side, or a left and a right side, the embryos are apparently formed bilaterally during embryogenesis. In order to facilitate descriptions, a dorso-ventral axis for the embryo was tentatively defined. The cells of the vermiform were named in accordance with the nomenclature of earlier authors [14, 16].

Terminology for identification of cells

At the two-cell stage, the two cells are designated A and B. Cell A divides and produces two daughter cells. One is designated 2a, the prospective axial cell, while the other is designated as 2A, the mother cell of peripheral cells. The first digit is equal to the cell generation, namely, the number of prior cell divisions. At the four-cell stage, two daughter cells of cell B are situated on the tentatively defined left and right sides of the embryo. The cell on the right side is distinguished from the cell on the left by underlining. Thus, the left and right cells are designated as 2B and 2B, respectively. Cell 2B produces two daughter cells. The anterior cell is designated 3B¹ and the posterior one is designated 3B². Thus, the anterior and posterior daughter cells of 3B¹ are designated 3B¹¹ and 3B¹², respectively.

RESULTS

At the nematogen stage, an agamete divides equally and produces two separate daughter agametes. They increase in number by mitosis, and some of them develop asexually into vermiform embryos within the axial cell of the nematogen (Figs. 1, 2a, and 8a).

Dicyema acuticephalum; the type with 16 peripheral cells (Figs. 2, 3, 4, and 5)

Before the first division, an agamete occasionally undergoes an extremely unequal division (Fig. 3a). The resultant much smaller cell remains attached to the larger one but it ultimately degenerates without contributing to embryogenesis. The first division is meridional and equal, producing two daughter cells, A and B (Fig. 3b). Cell B is the

mother cell of the head peripheral cells. The second division involves only cell A. This division is latitudinal and equal, producing two daughter cells, 2A and 2a (Figs. 3c and d). Cell 2A is the mother cell of the peripheral cells of the trunk and tail, while cell 2a is the prospective axial cell. The third division involves cell B. This division is meridional and equal, producing two daughter cells, 2B and 2B (Fig. 3e). At this four-cell stage, two pairs of cells, 2A-2a and 2B-2B, are arranged crosswise with respect to one another. The third division furrow coincides with the plane of bilateral symmetry of the embryo. The pattern of division and the cell lineage of descendants of cell 2B are the same as those of cell 2B.

The fourth division involves at cell 2A. This division is also meridional and equal, resulting in the five-cell stage (Figs. 3f-h). The division plane again coincides with the plane of bilateral symmetry and it separates the right cell (3A) from the left cell (3A). The division pattern and the cell lineage of descendants of cell 3A are the same as those of cell 3A. At around the five-cell stage, cell 2a, the prospective axial cell, undergoes an extremely unequal division and produces two daughter cells that are quite different in size (Figs. 3i and j). The larger cell, 3a, retains the characteristic of the parent cell, while the much smaller cell degenerates and ultimately disappears during embryogenesis. Cell 3a gradually becomes larger prior to the next division.

The pattern of cell division beyond the five-cell stage changes from spiral to bilateral. After the five-cell stage, divisions occur not one by one but in pairs, and they become almost synchronous. Therefore, subsequent developmental stages proceed with odd numbers of cells, yielding, for example, a seven-cell stage, and so on. The fifth division is an equal division and results in the seven-cell embryo (Figs. 3k and l). Thus, cells 2B and 2B divide and produce two pairs of daughter cells, 3B¹ and 3B² plus 3B¹ and 3B², respectively. The future anterior-posterior axis of the embryo corresponds almost exactly to the 3B¹-3A axis of the seven-cell embryo. The sixth division is extremely unequal (Fig. 3m). Cells 3B¹ and 3B¹ divide and together they produce a pair of large cells and a pair of much smaller

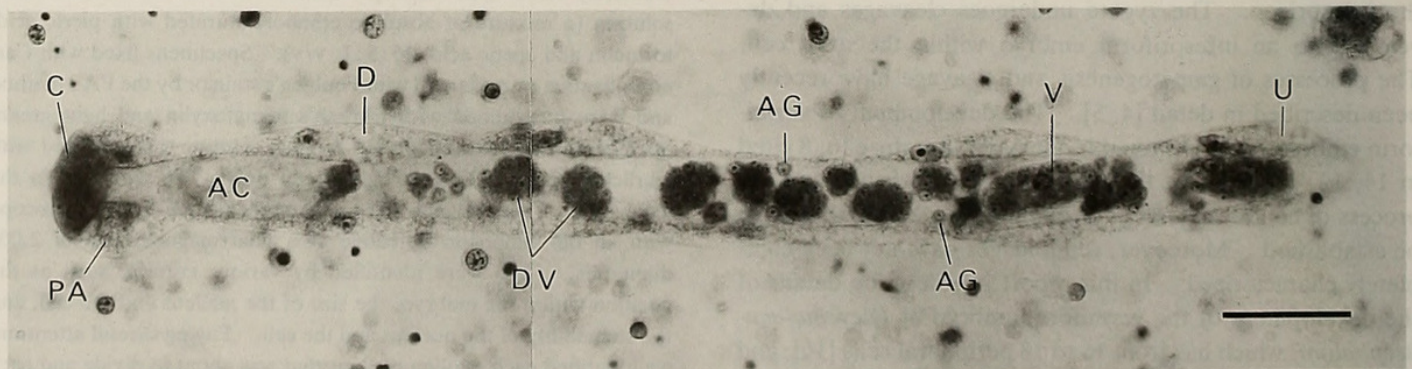


FIG. 1. Light micrograph of a nematogen of *Dicyema japonicum*. Scale bar represents 50 μ m. Abbreviations for this and subsequent Figures (Figs. 2-4, 6, 8-10): AC, axial cell; AG, agamete; C, calotte; D, diapolar cell; DV, developing vermiforms; M, metapolar cell; N, nucleus of the axial cell of a nematogen; P, propolar cell; PA, parapolar cell; PAC, prospective axial cell; U, uropolar cell; V, fully formed vermiform.

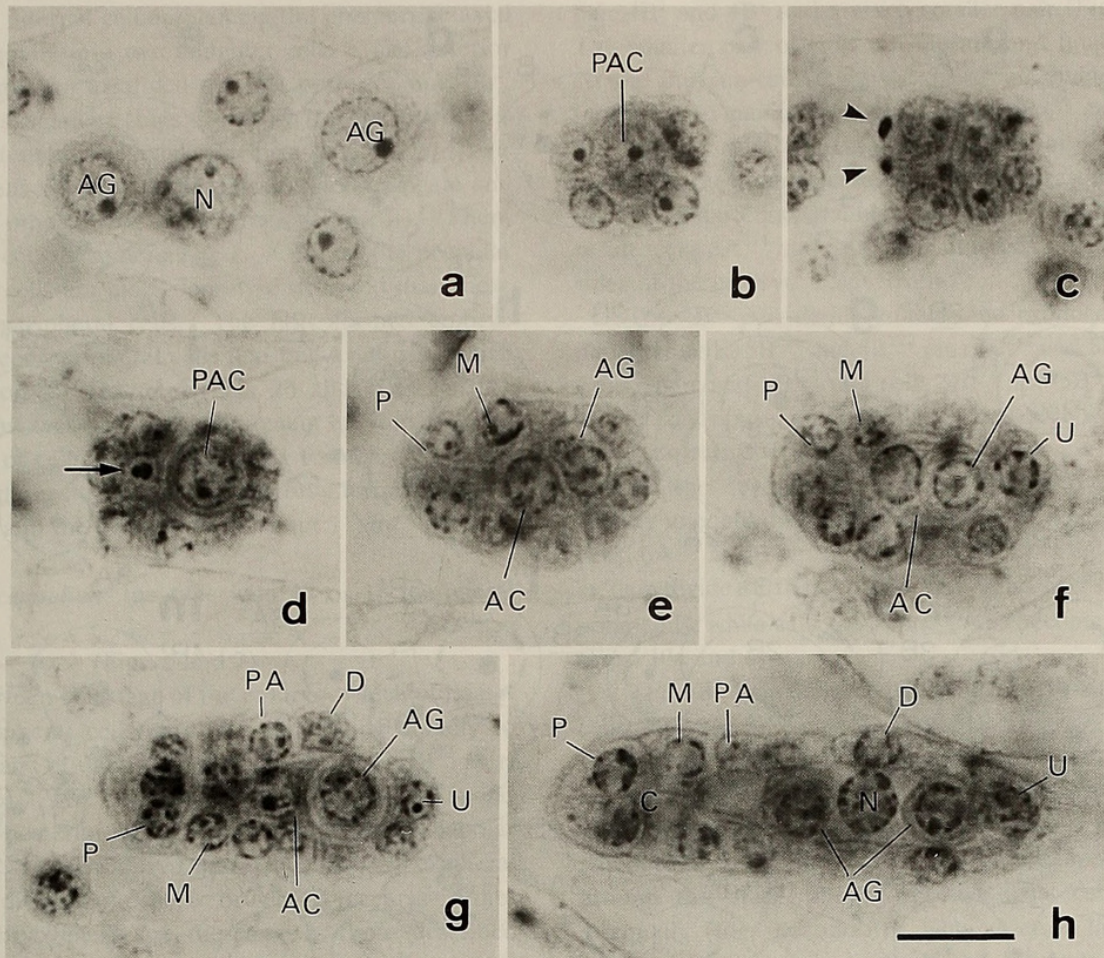


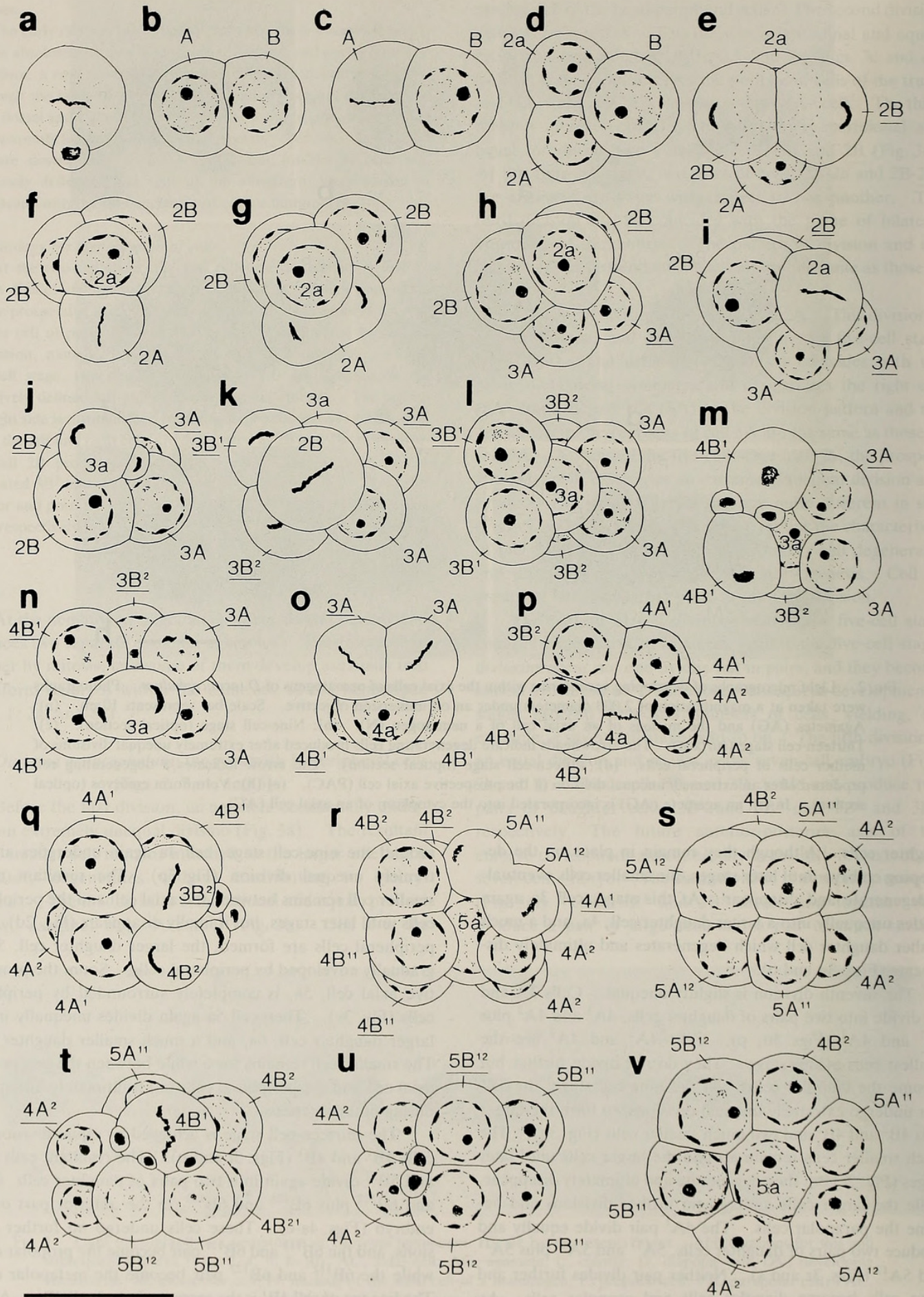
FIG. 2. Light micrographs of developing vermiforms within the axial cells of nematogens of *D. acuticephalum*. Photographs were taken at a magnification of 2,000 diameters under an oil immersion objective. Scale bar represents $10\mu\text{m}$. (a): Agametes (AG) and the nucleus of an axial cell of a nematogen (N). (b): Nine-cell stage (optical section). (c): Thirteen-cell stage (surface). The arrowheads indicate degenerating cells produced after extremely unequal divisions of mother cells of peripheral cells. (d): Fifteen-cell stage (optical section). The arrow indicates a degenerating cell produced after an extremely unequal division of the prospective axial cell (PAC). (e)-(h): Vermiform embryos (optical section). In (f), an agamete (AG) is incorporated into the cytoplasm of an axial cell (AC).

daughter cells. Although they remain in place on the developing embryo until later stages, the smaller cells eventually degenerate and disappear. At this stage, cell 3a again divides unequally into a larger daughter cell, 4a, and a much smaller daughter cell which degenerates and ultimately disappears (Figs. 3n and o).

The seventh division is slightly unequal. Cells 3A and 3A divide into two pairs of daughter cells, $4A^1$ and $4A^2$ plus $\underline{4A^1}$ and $\underline{4A^2}$ (Figs. 3o, p). Cells $\underline{4A^1}$ and $\underline{4A^2}$ are the smallest cells at this stage. They do not divide further but become the diapolar cells. At the nine-cell stage, the $3B^2$ pair undergo extremely unequal divisions, to form the larger cells $4B^2$ and $\underline{4B^2}$ and two much smaller cells (Fig. 3q). The much smaller cells remain around the larger cells until later stages (Fig. 2c) but they degenerate and ultimately disappear, while the larger cells undergo no further divisions and become the parapolar cells. The $4A^1$ pair divide equally and produce two pairs of daughter cells, $5A^{11}$ and $5A^{12}$ plus $\underline{5A^{11}}$ and $\underline{5A^{12}}$ (Figs. 3r and s). Neither pair divides further and these cells become diapolar cells and uropolar cells. At

around the nine-cell stage, cell 4a again undergoes an extremely unequal division (Fig. 3p). The resultant much smaller cell remains between the axial cell and the peripheral cells until later stages, but it finally disappears (Fig. 2d). As peripheral cells are formed, the larger daughter cell, 5a, is gradually enveloped by peripheral cells. Soon, the prospective axial cell, 5a, is completely surrounded by peripheral cells (Fig. 3v). Then cell 5a again divides unequally into a larger daughter cell, 6a, and a much smaller daughter cell. The smaller cell remains for a while between the prospective axial cell and the peripheral cells but it ultimately disappears during embryogenesis.

The thirteen-cell stage is achieved by equal divisions of cells $4B^1$ and $\underline{4B^1}$ (Figs. 3t and u). The resultant cells $5B^{11}$ and $5B^{12}$ divide again into two pairs of daughter cells, $6B^{111}$ and $6B^{112}$ plus $6B^{121}$ and $6B^{122}$, in the anterior part of the embryo (Figs. 4a-e). These cells undergo no further divisions, and the $6B^{111}$ and $6B^{121}$ pair become the propolar cells, while the $6B^{112}$ and $6B^{122}$ pair become the metapolar cells. The lineage of cell $4B^1$ is the same as that of cell $\underline{4B^1}$. At the



same time, the internal cell 6a, namely the prospective axial cell, divides equally into two daughter cells. The anterior cell, $7a^1$, becomes an axial cell and the posterior one, $7a^2$, becomes the first agamete (Figs. 2e and 4b). The agamete is soon incorporated into the axial cell (Figs. 2e and f). A pair of parapolar cells situated in the dorsal region elongate and approach each other in the ventral region (Fig. 4f). Then, the peripheral cells become ciliated. Cilia on the propolar and metapolar cells are more densely distributed than those on the other peripheral cells. The fully formed embryo consists of sixteen peripheral cells and one axial cell, which contains two to four agametes (Figs. 2h and 4f). Further development involves only the enlargement and intracellular differentiation of cells that have already formed (Fig. 2f-h). The body length, excluding cilia, of the fully formed embryo is about $55\mu\text{m}$ and the body width is about $11\mu\text{m}$.

Dicyema acuticephalum; the type with 17 or 18 peripheral cells

(Figs. 6 and 7)

At the thirteen-cell stage of the embryo, which ultimately has 18 peripheral cells, the $4B^2$ pair divide equally to produce two pairs of daughter cells, the $5B^{21}$ and $5B^{22}$ pairs (Figs. 6a and b). The anterior $5B^{21}$ pair become parapolar cells, while the posterior $5B^{22}$ pair become the fourth diapolar cells (Fig. 6c). In the embryo that finally has 17 peripheral cells, terminal division of cell $4B^2$ or cell $4B^2$ occurs. Other aspects of embryogenesis are the same as those described above for *D. acuticephalum* with 16 peripheral cells.

Dicyema japonicum

(Figs. 8, 9, 10, and 11)

Up to the nine-cell stage, the pattern of development and the cell lineage in *D. japonicum* are the same as those described for *D. acuticephalum*. In the 2a line, extremely unequal divisions occur at around the five-, seven-, nine-, and seventeen-cell stages (Figs. 8c, d and 11).

At the eleven-cell stage, in *D. japonicum*, the $3B^2$ pair of cells divide equally into $4B^{21}$ and $4B^{22}$ pairs (Figs. 9a-c). Almost simultaneously, the cells of the $3B^1$ pair undergo extremely unequal divisions, generating the larger daughter

pair $4B^1$ and $4B^1$ and a much smaller pair (Figs. 9d and e). The smaller pair of cells degenerate and finally disappear. At the thirteen-cell stage, the $5A^{11}$ pair divide equally and produce two pairs of daughter cells, $6A^{111}$ and $6A^{112}$ plus $6A^{111}$ and $6A^{112}$ (Fig. 9f). The plane of this division is parallel to the antero-posterior axis in contrast to the previous division that occurs parallel to the dorso-ventral axis. As the result, cells $6A^{111}$ and $6A^{111}$ are situated on the left and right sides of the embryo, respectively.

The $4B^{22}$ pair divide equally and produce two pairs of daughter cells, $5B^{221}$ and $5B^{222}$ plus $5B^{221}$ and $5B^{222}$ (Fig. 9g). Cells $5B^{221}$ and $5B^{221}$ and cells $5B^{222}$ and $5B^{222}$ undergo no further divisions and become parapolar cells and diapolar cells, respectively (Figs. 10a and c).

At the seventeen-cell stage, the $5A^{12}$ pair undergo slightly unequal divisions and produce two pairs of daughter cells, $6A^{121}$ and $6A^{122}$ plus $6A^{121}$ and $6A^{122}$ (Fig. 9h). Neither pair divide further. Cells $6A^{121}$ and $6A^{121}$ become uropolar cells, while cells $6A^{122}$ and $6A^{122}$ become diapolar cells (Figs. 10a and c).

The $4B^1$ pair divide equally into two pairs of daughter cells, $5B^{11}$ and $5B^{12}$ plus $5B^{11}$ and $5B^{12}$ (Figs. 9i and j). Soon after these divisions, the $4B^{21}$ pair divide equally into two pairs of daughter cells, $5B^{211}$ and $5B^{212}$ plus $5B^{211}$ and $5B^{212}$ (Figs. 9k and l). $5B^{211}$ and $5B^{211}$ become propolar cells, while cells $5B^{212}$ and $5B^{212}$ become metapolar cells. At around this stage, the prospective axial cell, 6a, divides unequally (Figs. 8e and f). The anterior large cell, $7a^1$, undergoes no further divisions and becomes an axial cell, while the posterior small cell, $7a^2$, becomes an agamete and is soon incorporated into the axial cell (Figs. 8g, h, and 10b). A pair of parapolar cells, situated in the dorsal region, elongate and approach each other in the ventral region (Figs. 10a and c). The vermiform embryo finally consists of twenty-two peripheral cells and one axial cell, which contains one or two agametes (Fig. 8i). The body length, excluding cilia, of the fully formed embryo is about $65\mu\text{m}$ and the body width is about $12\mu\text{m}$. No variations in cell lineage were found among embryos examined.

FIG. 3. Sketches of early embryos of *Dicyema acuticephalum*. Scale bar represents $10\mu\text{m}$. (a): An agamete undergoing an extremely unequal division. This division is not always seen. (b) and (c): Two-cell stage. In (c), a metaphase figure in cell A is depicted. This division produces a prospective axial cell (2a) and a mother cell of peripheral cells (2A). (d) and (e): Three-cell stage. In (e), a telophase figure in cell B is depicted. This division produces a mother cell of the left head (2B) and of the right head (2B). (f) and (g): Four-cell stage. In (f), a metaphase figure in cell 2A is shown. In (g), an anaphase figure in cell 2A is depicted. This division produces a mother cell of the left trunk (3A) and of the right trunk (3A). (h)-(k): Five-cell stage. In (i), a metaphase figure in cell 2a is shown. In (j), a telophase figure in cell 2a is depicted. This extremely unequal division produces cell 3a and a much smaller cell which is destined to die. In (k), the left (2B) and right cell (2B) divide almost synchronously. (l)-(o): Seven-cell stage. In (m), cells $3B^1$ and $3B^1$ undergo an extremely unequal division to produce cells $4B^1$ and $4B^1$ and two much smaller cells which are destined to die. In (n), cell 3a undergoes an extremely unequal division. In (o), metaphase figures in cells 3A and 3A are shown. (p)-(r) Nine-cell stage. In (p), a metaphase figure (lower center) in cell 4a is depicted. In (q), a metaphase figure in cell $3B^2$ (upper right) and a telophase figure (lower right) in cell $3B^2$ are shown. The cell divisions are extremely unequal. In (r), an anaphase figure (upper right) in cell $4A^1$ is shown. This equal division produces cells $5A^{11}$ and $5A^{12}$. (s): Eleven-cell stage. (t): Twelve-cell stage. Note a metaphase figure in cell $4B^1$ that is dividing equally to produce cells $5B^{11}$ and $5B^{12}$. (u): Thirteen-cell stage (surface view). (v): Thirteen-cell stage (sagittal optical section).

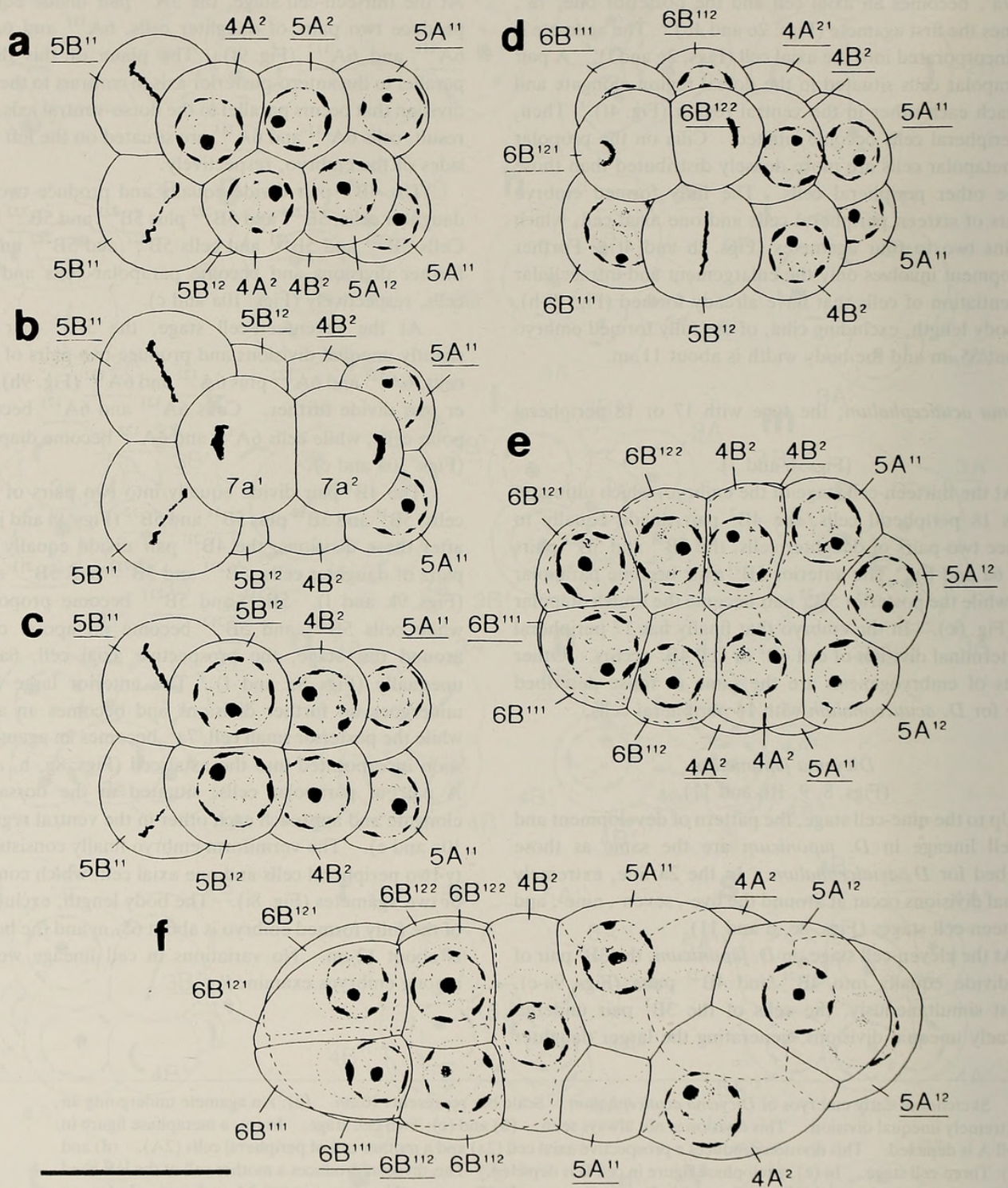


FIG. 4. Sketches of late embryos of *D. acuticephalum*. Scale bar represents $10\mu\text{m}$. (a): Thirteen-cell stage (ventral view). Note metaphase figures in cells $5B^{11}$ and $5B^{11}$ that are dividing equally to produce propolar cells and metapolar cells. (b): Thirteen-cell stage (horizontal optical section). Note a telophase figure in cell $6a^1$. This division produces an axial cell ($7a^1$) and the first agamete ($7a^2$). (c): Thirteen-cell stage (dorsal view). (d): Fifteen-cell stage (dorsal view). Cell $5B^{12}$ divides equally to produce a propolar cell and a metapolar cell. (e): Nearly formed embryo (lateral view). (f): Fully formed embryo (lateral view). Cilia have been omitted.

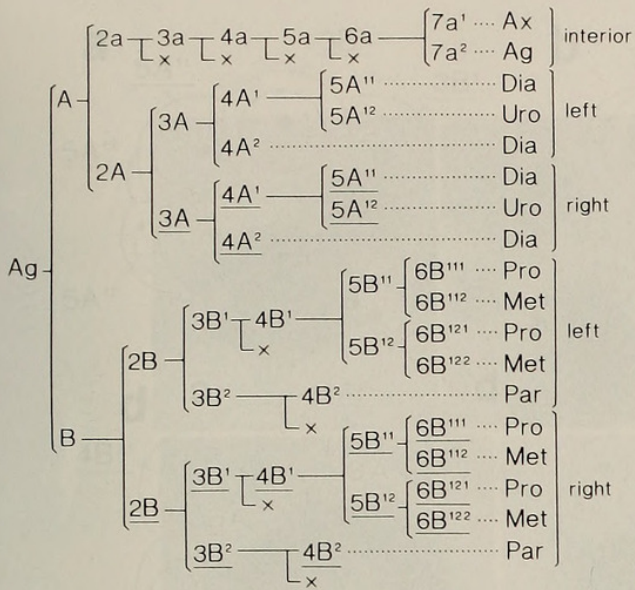


FIG. 5. Cell lineage of the vermiform embryo of *Dicyema acuticephalum* that has sixteen peripheral cells. A cross (x) indicates that a cell, formed as the result of an extremely unequal division, degenerates and does not contribute to the formation of the embryo. Abbreviations in Figs. 5, 7, and 11: Ag, agamete; Ax, axial cell; Dia, diapolar cell; Par, parapolar cell; Pro, propolar cell; Met, metapolar cell; Uro, uropolar cell.

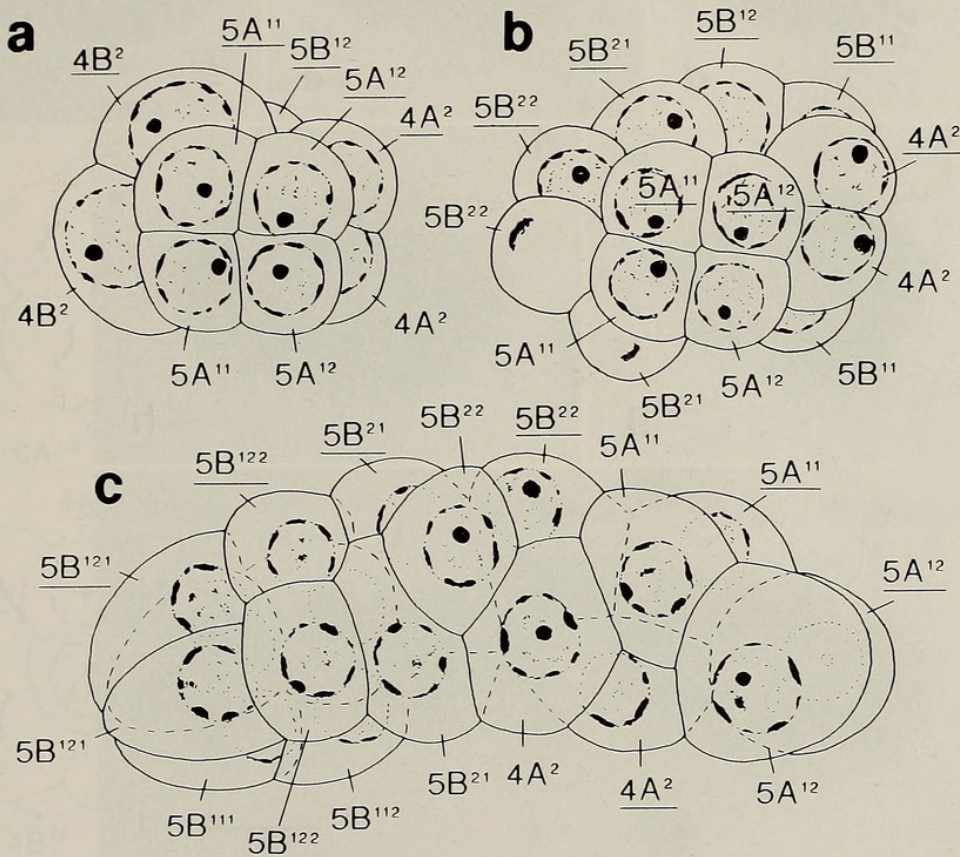


FIG. 6. Sketches of late embryos and a fully formed embryo of *Dicyema acuticephalum* that has eighteen peripheral cells. Scale bar represents 10 μm. (a): Thirteen-cell stage (from the tail). (b): Fourteen-cell stage (from the tail). Note a telophase figure in cell 4B². This division produces a parapolar cell (5B²¹) and a diapolar cell (5B²²). (c): Fully formed embryo. Cilia have been omitted.

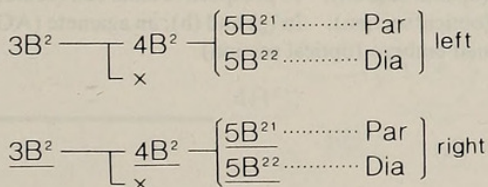


FIG. 7. The lineage of cells 3B² and 4B² of the vermiform embryo of *Dicyema acuticephalum* that has eighteen peripheral cells. The other aspects of cell lineage are the same as those of *D. acuticephalum* with sixteen peripheral cells. See the legend to Fig. 5 for abbreviations.

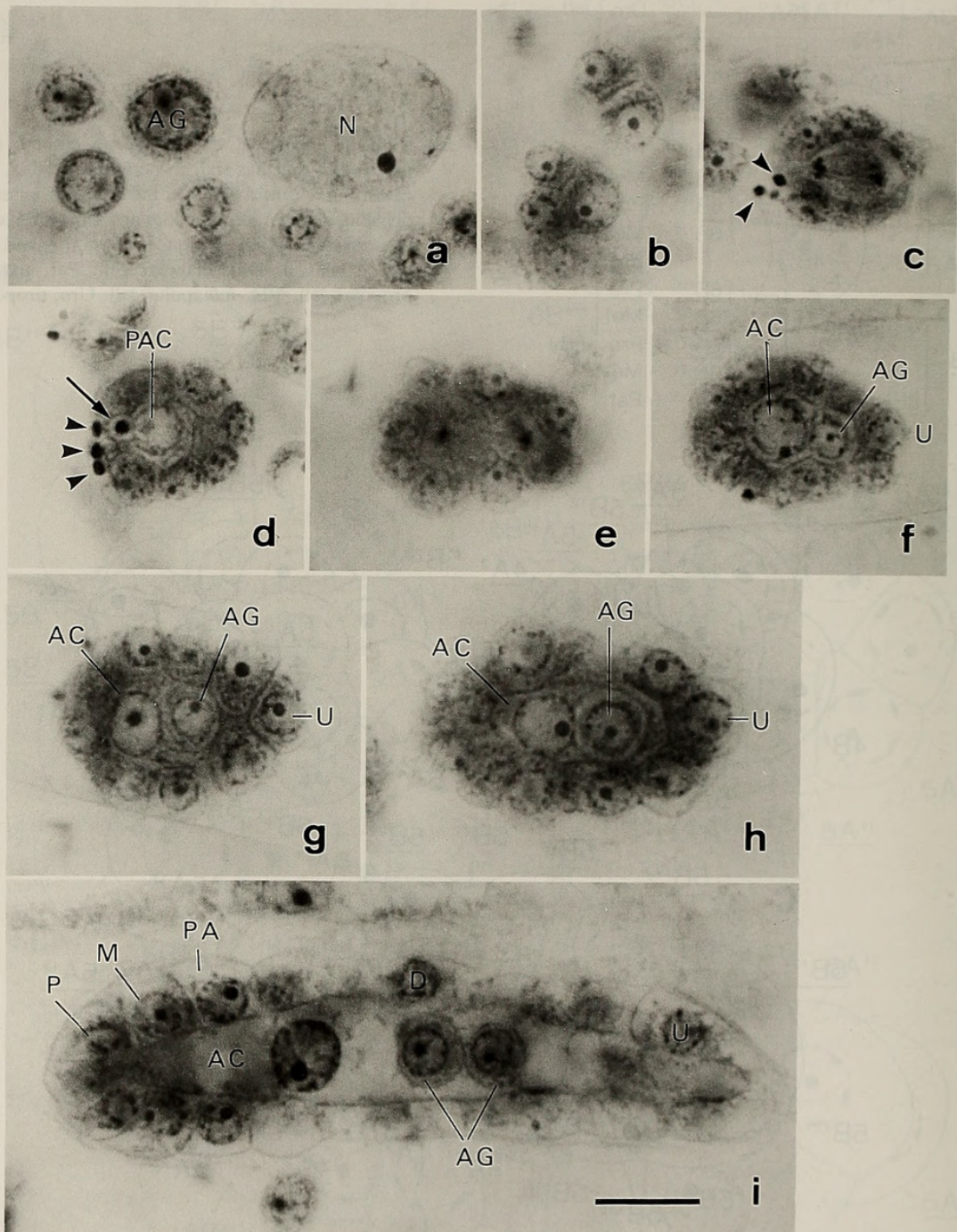
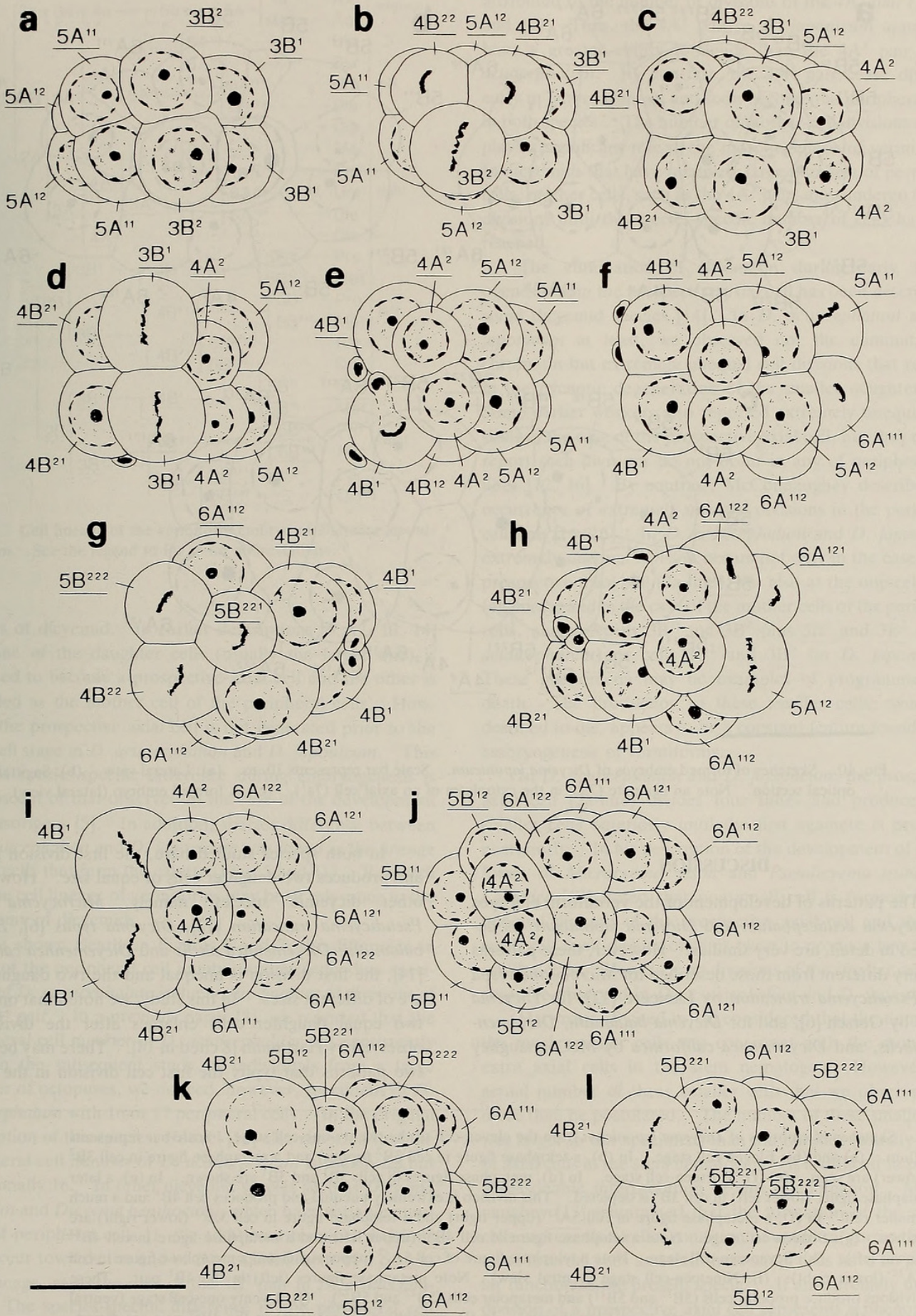


FIG. 8. Light micrographs of developing vermiform embryos within the axial cells of nematogens of *D. japonicum*. Scale bar represents $10\mu\text{m}$. (a): An agamete (AG) and the nucleus (N) of an axial cell of a nematogen. (b): Two-cell stage (upper) and three-cell stage (lower). (c): Thirteen-cell stage (optical section). A prospective axial cell (center) is undergoing an extremely unequal division. The arrowheads indicate degenerating cells produced after extremely unequal divisions. (d): Fifteen-cell stage (optical section). The arrowheads indicate degenerating cells produced after extremely unequal divisions of peripheral cells, while the arrow indicates a degenerating cell produced after an extremely unequal division of a prospective axial cell (PAC). (e): Seventeen-cell stage (optical section). A prospective axial cell (center) is undergoing an unequal division. (f) to (h): Developing vermiforms (optical section). In (g) and (h), an agamete (AG) is incorporated in the cytoplasm of an axial cell (AC). (i): Fully formed embryo (optical section).



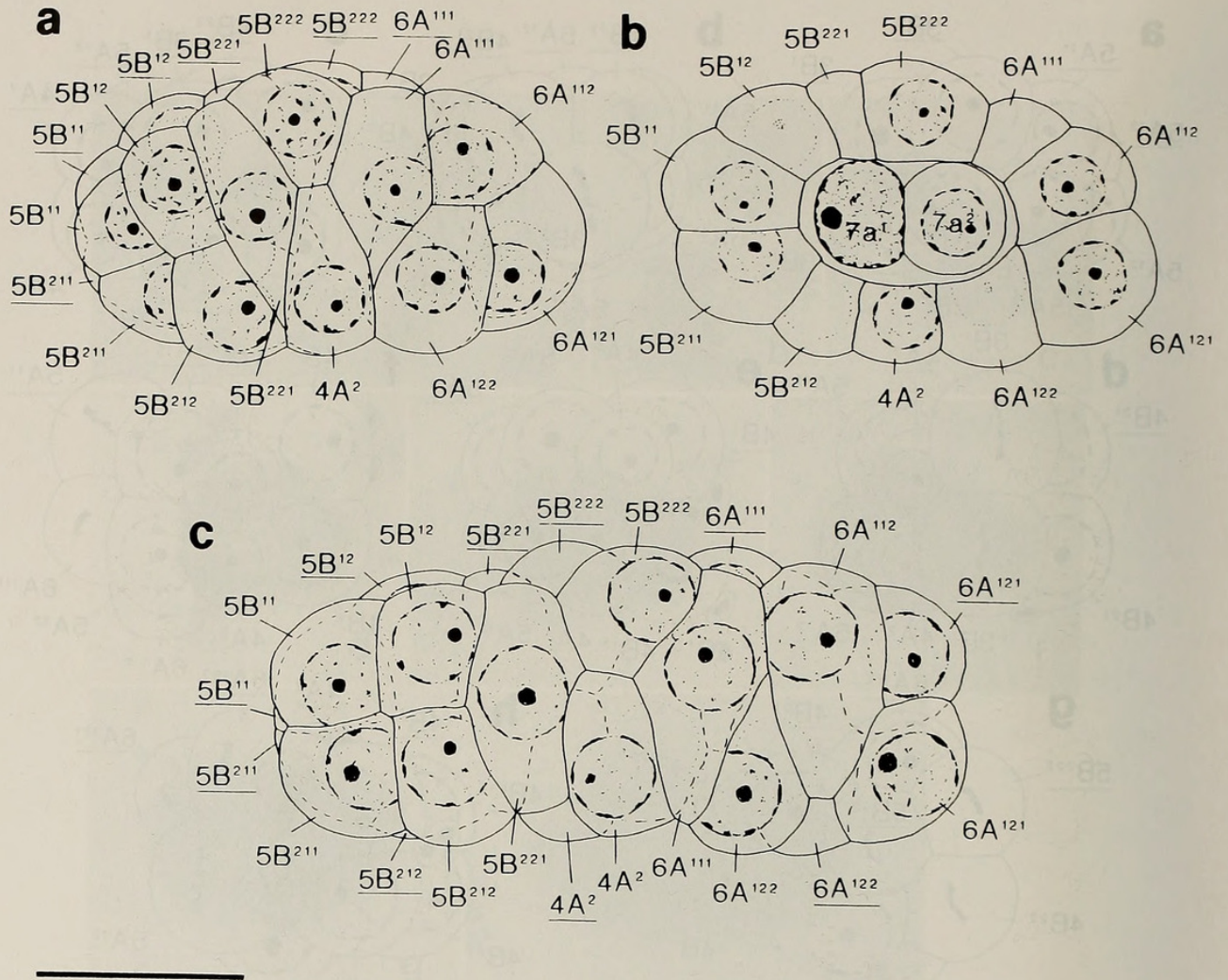


FIG. 10. Sketches of formed embryos of *Dicyema japonicum*. Scale bar represents $10\mu\text{m}$. (a): Lateral view. (b): Sagittal optical section. Note an agamete ($7a^2$) in the cytoplasm of an axial cell ($7a^1$). (c): A formed embryo (lateral view).

DISCUSSION

The patterns of development of the vermiform embryos of *Dicyema acuticephalum* and *Dicyema japonicum*, as described in detail, are very similar. However, these patterns are very different from those described for *Microcyema vespa* and *Pseudicyema truncatum* by Lameere [12], for *Dicyema typus* by Gersch [6], and for *Dicyema balamuthi*, *Dicyemennea abelis*, and *Dicyemennea californica* by McConnaughey [14].

In both species studied here, the first division is equal and produces two daughter cells of equal size. However, in other dicyemid species, namely, *Microcyema vespa*, *Pseudicyema truncatum* [12], *Dicyema typus* [6], *Dicyema balamuthi*, *Dicyemennea abelis* and *Dicyemennea californica* [14], the first division is unequal and the two daughter cells are of different sizes. In this study, we noted that one of the two equal daughter cells enlarges after the division, as observed by Hartmann [8 cited in 14]. There may be at least two patterns that typify the first cell division in the various

FIG. 9. Sketches of embryos of *Dicyema japonicum* from the eleven-cell to the twenty-one-cell stage. Scale bar represents $10\mu\text{m}$. (a) and (b): Eleven-cell stage. In (b), a telophase figure in cell $3B^2$ (upper) and a metaphase figure in cell $3B^2$ (lower) are seen. (c)-(f): Thirteen-cell stage. In (d), metaphase figures in cells $3B^1$ and $3B^1$ are shown. In (e), a later anaphase figure (lower left) in cell $3B^1$ is depicted. This division is extremely unequal and produces cell $4B^1$ and a much smaller cell. In (f), a metaphase figure in cell $5A^{11}$ (upper right) and a telophase figure in cell $5A^{11}$ (lower right) are shown. (g): Sixteen-cell stage. Note a telophase figure of cell $4B^{22}$ (upper left) and a metaphase figure in cell $4B^{22}$ (lower left). (h): Seventeen-cell stage. Note a telophase figure of cell $5A^{12}$ (upper right) and a metaphase figure in cell $5A^{12}$ (lower right). (i): Nineteen-cell stage (ventral view). Note metaphase figures (left) in the $4B^1$ pair. These divisions produce propolar cells ($5B^{11}$ and $5B^{11}$) and metapolar cells ($5B^{12}$ and $5B^{12}$). (j): Twenty-one-cell stage (ventral view). (k) and (l): Twenty-one-cell stage (dorsal view). In (l), metaphase figures (left) in the $4B^{21}$ pair are shown. These divisions produce propolar cells ($5B^{211}$ and $5B^{211}$) and metapolar cells ($5B^{212}$ and $5B^{212}$).



Furuya, Hidetaka, Tsuneki, Kazuhiko, and Koshida, Yutaka. 1994. "The Development of the Vermiform Embryos of Two Mesozoans, *Dicyema acuticephalum* and *Dicyema japonicum*." *Zoological science* 11, 235–246.

View This Item Online: <https://www.biodiversitylibrary.org/item/125367>

Permalink: <https://www.biodiversitylibrary.org/partpdf/71349>

Holding Institution

Smithsonian Libraries and Archives

Sponsored by

Biodiversity Heritage Library

Copyright & Reuse

Copyright Status: In Copyright. Digitized with the permission of the rights holder.

License: <http://creativecommons.org/licenses/by-nc-sa/3.0/>

Rights: <https://www.biodiversitylibrary.org/permissions/>

This document was created from content at the **Biodiversity Heritage Library**, the world's largest open access digital library for biodiversity literature and archives. Visit BHL at <https://www.biodiversitylibrary.org>.